SIN-CHN
SCIENTIFIC PRESS PTE.LTD.

Molecular & Cellular Biomechanics 2024, 21(4), 502.
https://doi.org/10.62617/mcb502

Article

Optimizing physical education movements through biomechanical analysis: A new approach to reducing the risk of sports injuries

Xianqi Huo

Institute of Physical Education, Shangqiu Normal University, Shangqiu 476000, China; klxy126@126.com

CITATION

Huo X. Optimizing physical education movements through biomechanical analysis: A new approach to reducing the risk of sports injuries. Molecular & Cellular Biomechanics. 2024; 21(4): 502. https://doi.org/10.62617/mcb502

ARTICLE INFO

Received: 10 October 2024
Accepted: 5 November 2024
Available online: 24 December 2024

Abstract: Physical education is crucial for fostering student's health, fitness, and lifetime active behaviors. However, using inappropriate movement skills during Physical activity may raise the risk of sports injuries. Biomechanical analysis is a scientific approach to studying the movement of students that focuses on the forces and mechanics of physical activity. The study's goal is to develop physical education motions using biomechanical analysis and a deep learning (DL) method to reduce the risk of sports injury. This study proposed a novel turbulent flow of water-based adjustable long-short-term memory (TFW-ALSTM) to classify and predict the high risk of sports injuries. Using advanced motion capture data and biomechanical modeling techniques, the study identifies improper movement patterns that can lead to injury during common physical education activities. The data was preprocessed using normalization and Kalman filters to reduce noise from the data. Discrete wavelet transforms (DWT) to extract the features from preprocessed data. The system offers beneficial suggestions to enhance movement efficiency through biomechanical data analysis. Experimental results reveal that the suggested model achieves accuracy (98.2%), recall (97%), specificity (98.1%), and an F1-Score (98%), particularly in dynamic activities like running and leaping, reducing the risk of injury considerably to compare existing algorithms. The study emphasizes the significance of integrating biomechanical knowledge and prediction models to enhance injury prevention measures in physical education programs. This approach provides educators and coaches with a dependable and effective tool for ensuring safer and more efficient student engagement.

Keywords: physical education movements; biomechanical; risk of injuries; turbulent flow of water based adjustable long short term memory (TFW-ALSTM)

1. Introduction

The development of owning a talent that supports health and well-being does not only begin and finish with physical fitness, but with physical education (PE) [1]. Another major purpose of PE programs is to provide students with the knowledge and skills required to participate in physical activities safely. In this case, minimizing sports injuries is vital since they may preclude participation or exacerbate the impact of prolonged physical activity [2]. Considering that, one must have a good understanding of how some physical education exercises can decrease the risk of injury in sports. Sports injuries are a common thing, no matter the age, but kids and teens who take part in organized sports are most susceptible to sports injuries [3]. These wounds might be anything from little damages, sprains, and strains to more major diseases requiring extensive recuperation. According to research, many sports injuries can be avoided with the right training, technique, and understanding of the body's physics. Consequently, attention should be focused on injury prevention programs aimed at strengthening, flexibility, coordination, and balance [4].

There has recently been an increased interest in understanding the biomechanical aspects that contribute to sports-related injuries [5]. By studying how athletes perform a movement on the field of play and assessing the risk factors linked with poor technique. Reducing the risk of anterior cruciate ligament (ACL) tears and ankle injuries, for example, can be accomplished through a series of exercises that strengthen the core of the body, the portions that connect to the lower portion of the body, and how the individual lands after jumping [6]. Furthermore, the curriculum for physical education may contain injury prevention measures to develop lifelong habits, as well as a safer sporting environment. Educators can teach their students the value of warm-up exercises, and stretching that is sufficient enough to help them maintain physical health and prevent injuries. Physical education programs empower students to take control of their physical health by educating them on injuries and prevention techniques [7].

This research aims to prevent sports-related injuries by reducing injury risk prediction and classification by biomechanical analysis and optimizing physical education motions using the suggested TFW-ALSTM model.

The following parts address the remaining research: Section 2 summarizes earlier studies. The proposed approach is presented in Section 3. The outcomes of applying the method are examined and discussed in Section 4. Section 5 presents the study's conclusions.

2. Related works

An AI-driven approach for improving injury management by incorporating rest periods during athletes' recovery phases was introduced [8]. The program combined data analytics to track athletes' health, resulting in a predictive tool for preventive injury management. The program employed powerful machine learning algorithms to determine training patterns, treatment options, and injury risk. The model's excellent accuracy in forecasting injury risks informs targeted intervention measured, which considerably reduces injury occurrence.

Some new possibilities for further investigation into the detailed macroscopic behavior level analysis given for optimizing training and sports performance were established [9]. More interventional research was required to learn more about the usefulness of the evaluated tools in specific training scenarios, even if most of them, apart from Errorless Learning with Unprompted Response (EUR), were presented as potentially valuable tools for guiding decisions connected to training.

Includedboth general and comprehensive models, along with the primary techniques used to simulate the dynamics of muscle contraction and activation was determined [10]. Several models of the skeleton, musculoskeletal system, and neuromusculoskeletal system were identified, varying in complexity, accuracy, and computing efficiency. That wassignificant to mention the best model would vary according tothe goals of the target population, the level of detail in the anatomical structures provided, and the motion that was performed.

Based on wearable technology, providing data analysis on recovery from injuries and prevention of injuries in physical education instruction was proposed . Wearable technology was used to capture workout data in real-time from students,

including metrics like heart rate, volume, steps, and distance. Data mining and analysis techniques were utilized to examine the data and investigate topics connected to physical recovery and avoiding injury when data was transmitted to cloud servers through the Internet of Things technology.

A multi-feature fuzzy evaluation model based on artificial intelligence was proposed [10]. Evaluating Physical education teaching methods at colleges and universities. The framework incorporated fuzzy instructions and the modified cuckoo search optimization algorithm, taking into account management, instructor, and student opinion when determining final evaluation outcomes. The proposed model received high results in several categories, including skill performance (97.01%), learning progress (87.36%), and teaching efficiency (96.8%), proving its effectiveness when compared to traditional methods.

To determine the efficacy of physical activity and exercise as no pharmaceutical therapies for preventing cognitive decline and dementia in older persons. It examined [11] various physical activity programs and compared how open-skill exercise (OSE) and closed-skill exercise (CSE) affect cognitive performance. The data suggest that aerobic therapies, notably OSE, had a larger protective effect on cognitive functioning, emphasizing the importance of promoting physical exercise globally.

The independent connections between device-measured sedentary time (ST) physical activity (PA) and heart anatomical and functional geometry in teenagers were established [12]. Results from the Avon Longitudinal Study showed that higher ST was associated with increased left ventricular mass in females and poorer diastolic function in males, emphasizing the need for physical exercise for teenagers' cardiovascular health.

3. Methodology

Data was collected by advanced motion data to analyze running habits, injury frequencies, and perceived benefits. Normalization and noise reduction with Kalman filtering were accomplished through preprocessing. Discrete Wavelet Transforms (DWT) were used to perform feature extraction. TFW-ALSTM is proposed to classify and predict sports injury risks based on identified movement patterns.

3.1. Data collection

Data has been gathered from the Kaggle source [13]. The dataset provides a complete overview of competitive runners physical activity, focusing on critical metrics needed for injury prediction and performance evaluation. It includes general kilometers traveled, which reflect average training volume, as well as intensity zones such as km z3-four (moderate to high intensity), km z5-t1-t2 (threshold training), and km sprinting (excessive-intensity efforts). It also monitors the number of training sessions and includes various other factors such as sprint distance run, strength training time, and hours spent on alternate training, providing a comprehensive of training intensity and effectiveness. Subjective measures such as perceived exertion, perceived training success, and perceived recovery provide qualitative insights into the athletes' experiences, and the dataset also includes injury prediction metrics that assess how training volume, intensity, and recovery factors influence injury risk.

This wealth of data allows for a thorough investigation of the relationships between training features, athlete well-being, and performance outcomes, making it an invaluable resource for optimizing training regimens and developing injury-prevention techniques in compensative running.

3.2. Data preprocessing

Data preprocessing included normalization to scale data so that they are comparable afterward and Kalman filters to minimize noise and retain accurate motion capture data that can be used for analysis and as a means for prediction of injury.

3.2.1. Min-max normalization

This method recalculates new values for each score using the minimum and maximum scores. This approach lacks robustness because it is highly susceptible to anomalies. The min-max normalization score can be subtracted from 1 to convert distance values into similarity scores as shown in Equation (1).

$$m = \frac{(T - Min(T))}{(Max(T) - Min(T))} \tag{1}$$

3.2.2. Noise reduction using kalman filter

To increase the accuracy ofanalyzing movement in physical education, the Kalman filter is a mathematical technique that lowers noise in biomechanical data to estimate the state of a dynamic system.

According to the Kalman filter theory, the system that generates the signal w_{l+1} has to be filtered using the form shown in Equations (2) and (3).

$$w_{l+1} = e(w_l, v_l) + u_l \tag{2}$$

$$z_l = g(w_l, v_l) + x_l \tag{3}$$

Here, z is the process noise, u is the noisemeasurement,v is the system's input, and y is the measured output.$w$represents the internal state of the system. With covariance provided by matrix $R$and$Q$ respectively in Equation (4), these noise processes are assumed to be, with zero mean Gaussian processes.

$$u_l \sim \mathcal{M}(0, R) x_l \sim \mathcal{M}(0, Q) \tag{4}$$

The Kalman filter computes the state estimate $\widehat{w}$ and the indicate matrix of covariance $\hat{O}$for each time step. The state is predicted one step ahead of time using the framework model in Equation (1). The time update, or a priori estimate, obtained through this procedure is represented as $\hat{O}$.This is followed by the measurement update. As a result, posteriori estimates of $\widehat{w}$and $\hat{O}$are obtained, updating the priori estimation with measurements containing determined measurement noise in Equations (5)–(9). It's typical for observations in databases to be irregularly spaced out and infrequent. To address this, the filter performs several time updates for each measurement update. The posteriori estimate is identical to the previous estimation in time steps in the absence of measurements.

$$\bar{w}_l = \Phi_{l-1}\hat{w}_{l-1} + A_{l-1}v_{l-1} \tag{5}$$

$$O_l = \Phi_{l-1}O_{l-1}\Phi_{l-1}^S + R_{l-1} \tag{6}$$

$$L_l = \bar{O}_l G_l^S \left(G_l \bar{O}_l G_l^S + Q_l\right)^{-1} \tag{7}$$

$$\hat{w}_l = L_l(z_l - G_l\bar{w}_l) \tag{8}$$

$$\hat{O}_l = (J - L_l G_l)\bar{O}_l \tag{9}$$

$G$is a measurement matrix, whereas Φ represents the transition matrix's state. Assuming nonlinearity in the process and measuring equations, these matrices are usually time-variant, can be determined by transforming$e$ and $g$in Equations (2) and (3) at every interval around the latest estimate, which yields the Kalman Filter (KF).

3.3. Feature extraction using DWT

To solve issues with the short-time Fourier Transform's frequency and temporal resolution capabilities, it was created as an alternative. To be more precise, in contrast to the Short-Time Fourier Transform (STFT), the DWT offers low and high resolution of regularity for high rates, as well as low and highresolution of datafor low occurrences. It is comparable in that regard, as both have comparable resolution features.

A specific example of the WT, the Discrete Wavelet Transform (DWT) offers an effectively computed compact way to represent a motion in period and rate. The following Equation (10) defines the DWT.

$$X(i,l) = \sum_i \sum_l w(l) 2^{-\frac{i}{2}} \psi(2^{-i}\, m - l) \tag{10}$$

where $\psi(s)$ is the mother wavelet, a finite energy interval function with rapid decay. An efficient, pyramidal algorithm associated with multi-rate filter banks can be used to carry out the DWT analysis.

The DWT, being a multi-rate filter bank, will be perceived as a fixed$R$filter bank where the filter centers are spaced one octave apart. Every half of each sample of the adjacent with a higher frequency, the pyramidal method breaks down into an initial approximation and detailed information, allowing for analysis of various frequencies and resolutions. Afterward, a second wavelet decomposition process is applied to further break down the initial approximation. This is specified by Equations (11) and (12)and is accomplished by filtering.

$$z_{high}[l] = \sum_m w[m]h[2l - m] \tag{11}$$

$$z_{low}[l] = \sum_m w[m]g[2l - m] \tag{12}$$

where, after being subsampled by, $z_{high}[l]$, $z_{low}[l]$, the quantity of wavelet coefficients produced and the number of input points are exactly equal as a result of the down-sampling.

3.4. Turbulent flow of water-based adjustable long-short-term memory (TFW-ALSTM)

To maximize biomechanical analysis in physical education, the Turbulent Flow of Water-Based Adjustable Long-Short-Term Memory (TFW-ALSTM) model integrates advanced deep learning with fluid dynamics concepts. TFW allows the model to accurately represent complex and flexible movement patterns by simulating the chaotic and adaptable features of turbulent water flow. At the same time, ALSTM improves on conventional Long Short-Term Memory systems by adding tunable parameters that maximize learning according to certain data properties. When combined, TFW-ALSTM offers an advanced method for anticipating movements that carry a high risk of injury, hence lowering the likelihood of sports-related illnesses and encouraging safer sports practices. Algorithm 1 despite the process of TFW-ALSTM to reducing sports injury risk.

Algorithm 1 Turbulent Flow of Water-based Adjustable Long-Short-Term Memory (TFW-ALSTM)

```
import numpy as np
import tensorflow as tf
from tensorflow.keras.models import Sequential
from tensorflow.keras.layers import LSTM, Dense, Dropout
class TFW_ALSTM:
def __init__(self, input_shape, lstm_units, num_classes):
self.model = Sequential()
self.add_tfw_layer()
self.model.add(LSTM(lstm_units, input_shape = input_shape, return_sequences = True))
self.model.add(Dropout(0.2))
self.model.add(LSTM(lstm_units))
self.model.add(Dropout(0.2))
self.model.add(Dense(num_classes, activation = ''))
def add_tfw_layer(self):
pass
def compile_model(self, learning_rate):
self.model.compile(optimizer = tf.keras.optimizers.Adam(learning_rate = learning_rate),
loss = 'categorical_crossentropy',
metrics = ['accuracy'])
def fit(self, X_train, y_train, epochs, batch_size):
self.model.fit(X_train, y_train, epochs = epochs, batch_size = batch_size)
def predict(self, X_test):
return self.model.predict(X_test)
def preprocess_data(data):
normalized_data = normalize(data)
return normalized_data
def main():
motion_capture_data = load_data()
X_train, y_train = preprocess_data(motion_capture_data)
input_shape = (timesteps, features)
lstm_units = 64
num_classes = 3
tfw_alstm_model = TFW_ALSTM(input_shape, lstm_units, num_classes)
tfw_alstm_model.compile_model(learning_rate = 0.001)
```

Algorithm 1 (*Continued*)

$tfw\_alstm\_model.fit(X\_train, y\_train, epochs = 50, batch\_size = \mathbf{32})$
$X\_test = load\_test\_data()$
$predictions = tfw\_alstm\_model.predict(X\_test)$
$\boldsymbol{if}\_name\_ == "\_\_\boldsymbol{main}\_\_"$:
$main()$

3.4.1. Adjustable long-short-term memory (ALSTM)

ALSTM is a more advanced recurrent neural network. Compared with the RNN, its essence depends on the development of an understanding of the cell condition. The conditions which should be remembered and which should remain behind will depend on the LSTM's cell state. The RNN gradient's disappearing issue has been resolved. Input, output, and forget gates are the three gates that make up the hidden layer of an LSTM network. The input and output flows in and out of a memory cell are managed by input and output gates, respectively. Selectively forgetting the data in the cell's current state is the function of forgetting gates. Because of its intricate structure, the training period for the standard LSTM network is longer. The Adjustable Long Short-Term Memory network (ALSTM) is suggested, and the structure of LSTM is modified to achieve the goal of decreasing network training time without compromising accuracy. ALSTM integrates the input gate and forgets the gate into one single gate to simplify network complexity. **Figure 1** shows the ALSTM network's structure. The ALSTM formula and forward propagation, as seen in Equations (13)–(22).

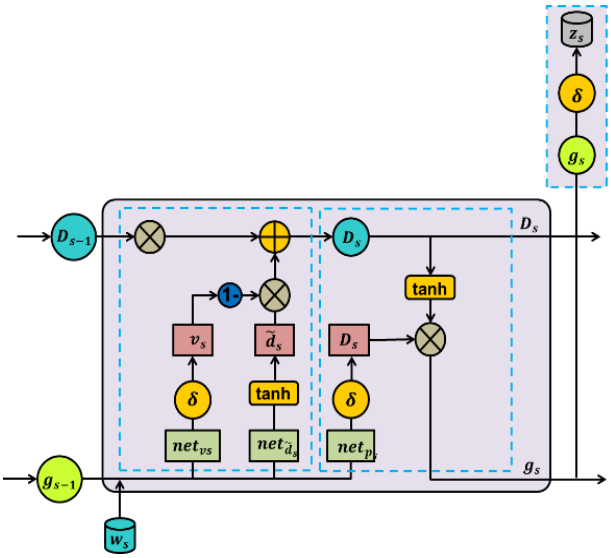

Figure 1. Overall structure of ALSTM.

Determine the shared gates represented in Equations (13) and (14)

$$net_{ut} = X_v.\begin{bmatrix} g_{s-1} \\ W_s \end{bmatrix} + a_v = X_{uh}.g_{s-1} + X_{ux}.w_s + a_v \tag{13}$$

$$v_s = \sigma(net_{ut}) \tag{14}$$

Determine the current condition of the information in Equations (15) and (16)

$$net_{\widetilde{ct}} = X_{\tilde{d}}.\begin{bmatrix} g_{s-1} \\ W_s \end{bmatrix} + a_d = X_{\widetilde{ch}}.g_{s-1} + X_{\widetilde{cx}}.w_s + a_{\tilde{d}} \tag{15}$$

$$\widetilde{d_s} = \tanh\left(net_{\widetilde{ct}}\right) \tag{16}$$

Upgrade the memory of the cell in Equation (17).

$$D_s = (1 - v_{s-1}) \times D_{s-1} + \widetilde{d_s} \times v_s \tag{17}$$

Determine the output gates in Equations (18) and (19).

$$net_{ot} = X_p \begin{bmatrix} g_{s-1} \\ W_s \end{bmatrix} + a_p = X_{oh}.g_{s-1} + X_{ox}.w_s + a_p \tag{18}$$

$$p_s = \sigma(net_{ot}) \tag{19}$$

Determine the hidden layer's output in Equation (20).

$$g_s = p_s \times \tanh\left(d_s\right) \tag{20}$$

Determine the predicted value's output in Equations (21) and (22).

$$y_s = X_z.g_s + a_z \tag{21}$$

$$z_s = \sigma(zt) \tag{22}$$

The current condition of the stage is represented by the formula above by the variables net_{ut}, $net_{\widetilde{ct}}$, net_{ot}, and y_s. They have weight matrices called X_v, X_d, and X_p. For the bias vectors, a_v,a_d, and a_p are used. In the current period, w_s, v_s, $\widetilde{d_s}$, and p_s represent the data states, output gates, shared gates, and input levels, in that order. The condition of the cells in both the earlier and later times is represented by D_s and D_{s-1}. Matrix multiplication is represented by the symbol . , while element-to-element multiplication is represented by the sign $\times$. $Tanh()$ and $Sigmoid()$ have different activation functions: $\tanh(w)$ and $\sigma(w)$, respectively. Here's an explanation of their estimated formula in Equation (23).

$$\begin{cases} \sigma(w) = z = \dfrac{1}{1 + e^{-w}} \\ \tanh(w) = z = \dfrac{e^{w} - e^{-w}}{e^{w} + e^{-w}} \end{cases} \tag{23}$$

The number of variables in the distribution of weights that need improvement is reduced when compared to ALSTM. Before updating the stored information cell, the ALSTM uses its activation function $Tanh(d_s)$ to activate the present information state. The current information state $\widetilde{d_s}$ and the prior cell memory D_{s-1} are then combined linearly, with update gate v_s serving as the significance of the available data $\widetilde{d_s}$ and $1 - v_s$ serving with the prior cell memory's quantity D_{s-1}. The sum of both values is a single one. Cell memory is updated in this way.

3.4.2. Turbulent flow of water (TFW)

A new metaheuristic algorithm is called Turbulent Flow of Water. It draws inspiration from the vortex phenomena that occur in a chaotic water flow. A vortex travels in a circle on a constricted path. A hole in the middle of the whirlpool drags

the surrounding particles toward it and subsequently pulls them into the vortex. The best member of every group is placed in thecenter of the whirlpool using the TFW algorithm, which divides the population into Non-Wetting Phase (NWh) groups.

- Formation And Effects of Whirlpools

The starting population (w^0), which consists of M_o members set equally, is divided among the NWh whirlpool by the method. Additionally, the positions of the items in a particular set (W) were merged with its center position by generating a centripetal impact on every whirlpool $M_{Wh}$and submerging them into its well. The W_j object location is then integrated with itself by every whirlpool ith (with its current position on Wh_i); this suggests that $(W_j = Wh_i)$. If this integration is not carried out, the gap $(W_j = Wh_i)$ between the objective values ($e()$) of other (Wh) whirlpools and those will cause some deviations (ΔW_j). Consequently, $W_j^{new} = Wh_i - \Delta W_j$ will be the object's jth new position. Furthermore, the unique angle (δ), which varies at each iteration in the following ways, limits the motion of the components (W) around the center and approach of their vortex represented in Equation (24).

$$\delta_j^{new} = \delta_j + rand_1 \times rand_2 \times \pi \tag{24}$$

Equations (25) and (26) have been used to determine the angle.

ΔW_j is based on the separation between the whirlpools and all of the items with the lowest and highest weights, respectively. After that, Equation (27) is used to update the particle's position.

$$\Delta_s = e(Wh_s) \times \left|Wh_s - sum(W_j)\right|^{0.5} \tag{25}$$

$$\Delta W_j = \Delta W_j = \left(\cos(\delta_j^{new}) \times rand(1, C) \times (Wh_e - W_j) - \sin(\delta_j^{new}) \times rand(1, C) \times (Wh_x - W_j)\right) \tag{26}$$

$$W_j^{new} = Wh_i - \Delta W_j \tag{27}$$

where the whirlpools with the lowest and highest values of Δ_s are Wh_e and Wh_X, respectively, and δ_j is the angle of the jth object.

- Mathematical Model

An outline of the TFW algorithm's mathematical steps is provided in this section.

- Updating object's position stage:

The updating of the object's location is described in the below two steps:

$Step\ 1$:

$$\text{for } s = 1\ M_{Wh}$$

$$\Delta_s = e(Wh_s) \times \left|Wh_s - sum(W_j)\right|^{0.5}$$

end

$$Wh_e = Wh_s with \min value\ of \Delta_s$$

$$Wh_x = Wh_s with \min value\ of \Delta_s$$

$$\delta_j^{new} = \delta_j + rand_1 \times rand_2 \times \pi$$

$$\Delta W_j = (\cos(\delta_j^{new}) \times rand(1, C) \times (Wh_e - W_j)$$

$$-\sin(\delta_j^{new}) \times rand(1, C) \times (Wh_x - W_j))$$

$$\times (1 + |\cos(\delta_j^{new}) \times -\sin(\delta_j^{new})|);$$

$$W_j^{new} = Wh_i - \Delta W_j;$$

$Step\ 2$:

$$W_j^{new} = \min\left(\max\left(W_j^{new}, W^{min}\right), W^{max}\right);$$

$$\text{if } e\left(W_j^{new}\right) <= e(W_j)$$

$$W_j = W_j^{new}$$

$$\text{e}\left(W_j\right) = e\left(W_j^{new}\right);$$

end

- The phase of centrifugal force

Accordingly, moving objects are pulled toward their whirlpool by the centripetal force FE_j, but occasionally FE_j is stronger than the whirlpool's centripetal force, causing the object to travel randomly to a new location. They are then moved away from the respective center by the centrifugal force. Additionally, the action and centrifugal force employ Equations (28) and (29), respectively. Furthermore, Step 3 provides a summary phase of the centrifugal force mathematical model.

$$FE_j = (\left(\left(\cos\left(\delta_j^{new}\right)\right)^2 \times \left(\cos\left(\delta_j^{new}\right)\right)^2\right)^2 \quad (28)$$

$$w_{j,o} = w_o^{min} + rand \times \left(w_o^{max} - w_o^{min}\right) \quad (29)$$

$Step\ 3$

$$FE_j = (\left(\cos\left(\delta_j^{new}\right)\right)^2 \times \left(\sin\left(\delta_j^{new}\right)\right)^2)^2$$

$$\text{if } rand < FE_j$$

$$\text{o} = round\left(1 + rand \times (C - 1)\right);$$

$$w_{j,o} = w_o^{min} + rand \times \left(w_o^{max} - w_o^{min}\right);$$

$$\text{e}\left(W_j\right) = e\left(W_j^{new}\right);$$

end

- Phase interactions among whirlpools

Whirlpools' effects on the objects have been analyzed. Similar to how a whirlpool affects nearby objects, every whirlpool tends to connect its location to the location of the whirlpool under consideration. Equation (30) is thus used to determine the minimal size of the closest whirlpool based on its goal function. The whirlpool position can be updated using Equations (31) and (32).

$$\Delta_s = e(Wh_s) \times |Wh_s - sum(Wh_i)| \quad (30)$$

$$\Delta Wh_i = rand(1, C) \times |\cos(\delta_i^{new}) + \sin(\delta_i^{new})| \times (Wh_e^{new} - Wh_i^{new}) \quad (31)$$

$$Wh_i^{new} = Wh_e - \Delta Wh_i \quad (32)$$

where δ acts on the value of the angle of the i^{th} whirlpool hole. It uses Steps 4 and 5, which show the relationship between the whirlpool interactions, to summarize the previous event.

$Step\ 4$

$$\text{for } s = 1: M_{Wh} - i$$

$$\Delta_s = e(Wh_s) \times |Wh_s - sum(Wh_i)|$$

end

$$Wh_e = Whwith \min valueof\ \Delta_s$$

$$Wh_i^{new} = Wh_e - \Delta Wh_i;$$

$$\Delta Wh_i = rand(1, C) \times |\cos(\delta_i^{new}) + \sin(\delta_i^{new})| \times (Wh_e^{new} - Wh_i^{new});$$

$$\delta_i^{new} = \delta_i + rand_1 \times rand_2 \times \pi$$

$Step\ 5$

$$Wh_i^{new} = \min\left(\max\left(Wh_i^{new}, W^{min}\right), W^{max}\right);$$

$$\text{if } e(Wh_i^{new}) \le e(Wh_i^{new})$$

$$Wh_i = Wh_i^{new};$$

$$\text{e}(Wh_i) = e(Wh_i^{new});$$

end

- The phase of the strongest members

The strongest member of the newly acquired whirlpool members is chosen for the subsequent iteration based on the objective function's lowest value about the relevant whirlpool. Step 6 shows the chosen new strongest whirlpool, summarizing this process.

$Step\ 6$

$$\text{if } e(W_{best}) \le e(Wh_i)$$

$$Wh_i \leftrightarrow W_{best}$$

end

4. Result

On Windows 11, Python 3.12 was utilized to complete tasks. The 12th generation Intel Core i7 processor had 32 GB of RAM. The device under review was a modern laptop setup that could evaluate performance under taxing multitasking and development tasks. The proposed approach, which uses biomechanical analysis

to optimize physical education movements, more accurately detects compliance problems than current injury risk methods like the Advanced penguin search optimized Efficient Random Forest (APSO-ERF) [14] and Adaboost algorithm and Random Forest (Ada-RF) [15]. During risk detection assessments, it produces metrics like accuracy (%), recall(%), specificity (%), and F1-score (%).

4.1. Confusion matrix

The performance of the classification model is shown by the confusion matrix, which has the following values: There were 8434 True Negatives (TN) indicating that students not at risk were accurately identified; 0 False Positives (FP) indicating that there were no incorrect at-risk predictions; 120 False Negatives (FN) demonstrating the incorrect identification of at-risk students; and 0 True Positives (TP) indicating that not at-risk students were correctly identified. There is potential for enhancement of the sensitivity of the model since this matrix shows good accuracy in identifying non-risk instances but indicates a considerable issue in identifying at-risk individuals, as shown in **Figure 2**.

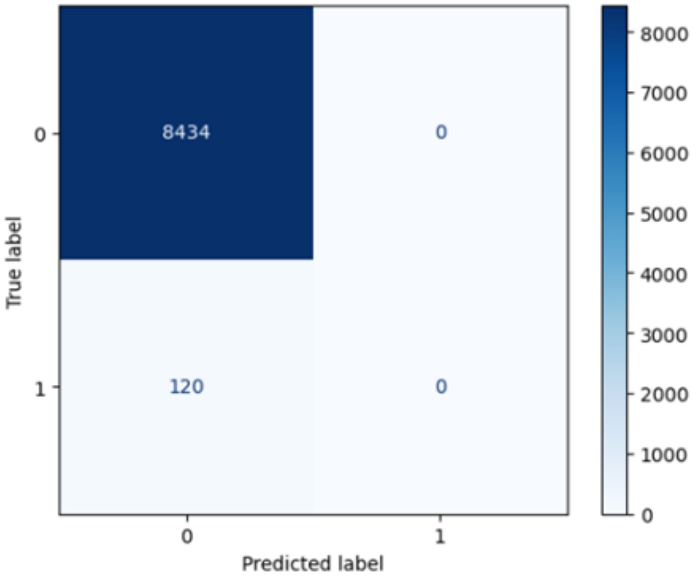

Figure 2. Confusion matrix of classification outcomes.

4.2. Performance in injury prevention

The proposed TFW-ALSTM model's performance indicators are shown in the graph, which also highlights the model's efficacy in injury prevention, injury prediction, and improved movement efficiency. The model shows notable improvements in safety and performance in physical education settings, with a 75% injury prediction rate, a 15% increase in movement efficiency, and a 20% decrease in injuries shown in **Figure 3**. Furthermore, these enhancements help to create safer environments for students while also promoting their overall physical well-being. By correctly recognizing capacity injury risks, the approach enables educators to implement timely interventions that also reduce injury rates during physical activities.

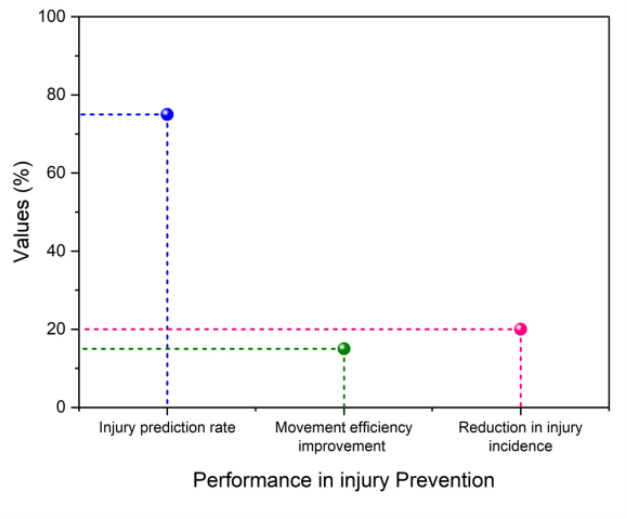

Figure 3. Outcomes in injury prevention performance.

4.3. Accuracy

Accuracy measures how close a measured value is to the true value. It assesses a model's or system's ability to correctly forecast outcomes and is commonly expressed as a percentage of accurate predictions overall total forecasts. The proposed TFW-ALSTM model is compared to existing methodologies to determine its capacity to accurately identify and explain sports injury compliance issues. A proposed TFW-ALSTM technique outperforms standard techniques significantly, with an accuracy value of 98.2% when compared to current models such as APSO-ERF (97.8%) and Ada-RF (86%). This demonstrates that the proposed method is a more sensible approach to detecting injury risks in physical education, and it encourages the development of an early warning system to increase student safety during physical activity. **Figure 4** and **Table 1** show the accuracy findings.

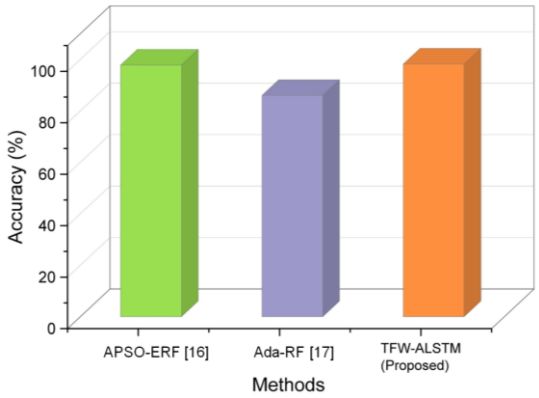

Figure 4. Accuracy of classification models.

Table 1. Performance metrics of classification algorithms.

Methods	F1-Score (%)	Specificity (%)	Recall (%)	Accuracy (%)
APSO-ERF [15]	97.5%	97.9%	96.1%	97.8%
Ada-RF [16]	68.3%	75.5%	88.5%	86%
TFW-ALSTM (Proposed)	98%	98.1%	97%	98.2%

4.4. Recall

Recall assesses a model's ability to correctly identify essential instances in a dataset. It is defined as the ratio of true positive forecasts to total real positives, and it measures how successfully the model recognises all key cases. Recall investigates the system's ability to recognize crucial movement patterns that indicate a student's risk of sports-related injury. The proposed TFW-ALSTM strategy had a take-into-recall rating of 97% when compared to other current methods, such as APSO-ERF and Ada-RF, which had considered rankings of 96.1% and 88.5%, respectively. This demonstrates that the suggested system outperforms cutting-edge methods for detecting potential capacity injury risks during physical training activities. **Figure 5** and **Table 1** present the result of recall.

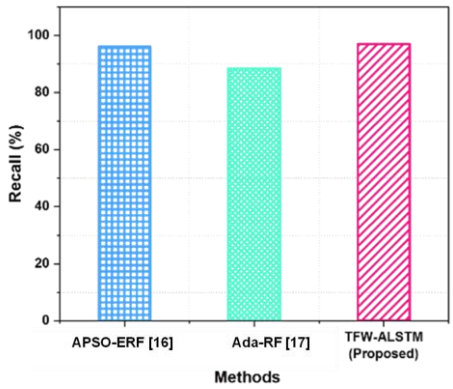

Figure 5. Recall of Classification models.

4.5. Specificity

Specificity refers to a model's ability to efficiently detect occurrences of negativity. It is expressed as the ratio of true negative forecasts to overall actual negatives. High specificity demonstrates that the methodology effectively minimizes false positive rates by differentiating applicable and irrelevant cases. Specificity measures how well the system detects instances that are not at risk of sports-related injuries. The proposed TFW-ALSTM strategy has a high specificity score of 98.1%, compared to existing methods such as APSO-ERF and Ada-RF, which have specificity values of 97.9% and 75.5%, respectively. This reveals that when it comes to accurately recognizing occurrences of student non-injury during physical education sports. **Figure 6** and **Table 1** show the effects of specificity.

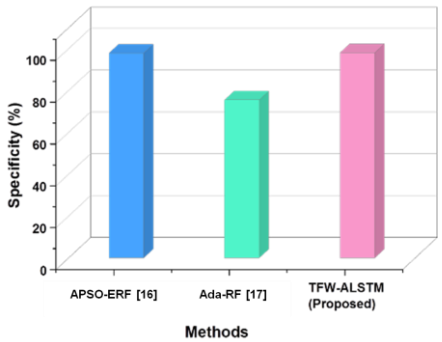

Figure 6. Specificity of classification models.

4.6. F1-score

The F1-score is a performance indicator that combines precision and recall ability into a single value, creating a balance of the two. It is calculated using the harmonic range of precision, which focusses the trade-off between erroneous positives and false negatives. An F1-score ranges from 0 to 1, with higher values indicating better overall model performance in reliably finding relevant cases. This measure allows us to compare the system's performance in identifying injury risks in physical education to that of different strategies like APSO-ERF and Ada-RF, which have F1 scores of 97.5% and 68.3%, respectively. Furthermore, the suggested TFW-ALSTM approach achieved an F1 score of 98%. This demonstrates that the proposed method performs much better than current methods in terms of accurately identifying students' risks of sports-related injuries. **Figure 7** and **Table 1** present the result of the F1score.

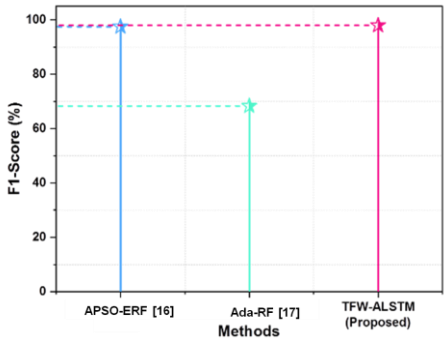

Figure 7. F1-score of classification models.

Table 1 compares the performance of three methods APSO-ERF, Ada-RF, and the proposed TFW-ALSTM model based on four metrics: F1-Score, Specificity, Recall, and Accuracy. The TFW-ALSTM outperforms other models, with the highest F1-score (98%), Specificity (98.1%), Recall (97%), and Accuracy (98.2%), showing its ability to detect relevant instances.

5. Conclusion

The study effectively demonstrated the efficacy of the Turbulent Flow of Water-primarily based Adjustable Long-Short-Term Memory (TFW-ALSTM) model in optimizing Physical education movements to reduce the risk of sports activities injuries. By utilizing higher biomechanical evaluation and deep learning methodologies, this study emphasizes the necessity of successfully identifying and correcting incorrect movement patterns that may cause injuries during physical activities. To reduce data noise, normalisation and Kalman filters were used during preprocessing. Discrete wavelet transformations (DWT) are used to extract features from preprocessed data. The results show that the TFW-ALSTM model significantly outperforms traditional injury risk assessment methodologies, attaining excellent metrics of 98.2% accuracy, 97% recall, 98.1% specificity, and an F1-score of 98 %. The limitations of this work include a highly confined and homogeneous dataset, which can also limit the TFW-ALSTM model's generalizability across more than

one demographic and physical activity. This study's challenges include a potentially limited sample size and diversity, a focus on specific activity, and assumptions made in biomechanical models. Future studies should include more activity analysis, wearable technology for real-time feedback, and longitudinal studies to assess long-term impact. Furthermore, cross-validation with other algorithms should improve the model's reliability, and personalizing biomechanical suggestions based on character profiles may increase applicability, ensuring more secure and efficient participation in physical education applications.

Ethical approval: Not applicable.

Conflict of interest: The author declares no conflict of interest.

Reference

1. Towner, B.C., Broce, R.S., Battista, R.A. and Christiana, R.W., 2024. A forced shift: Effects and outcomes of online higher education physical activity courses. International Journal of Kinesiology in Higher Education, 8(1), pp.24-36.
2. Hao, Q., Choi, W.J. and Meng, J., 2023. A data mining-based analysis of cognitive intervention for college students' sports health using Apriori algorithm. Soft Computing, 27(21), pp.16353-16371.
3. Cui, J., Du, H. and Wu, X., 2023. Data analysis of physical recovery and injury prevention in sports teaching based on wearable devices. Preventive medicine, 173, p.107589.
4. dos Santos Duarte Junior, M.A., López-Gil, J.F., Caporal, G.C. and Mello, J.B., 2022. Benefits, risks, and possibilities of strength training in school Physical Education: a brief review. Sport Sciences for Health, pp.1-10.
5. Hughes, G. and Dai, B., 2023. The influence of decision making and divided attention on lower limb biomechanics associated with anterior cruciate ligament injury: a narrative review.Sports biomechanics,22(1), pp.30-45.
6. Hosseinimehr, S.H. and Salvati, F., 2024. Improving lower limb muscle strength according to a number of weeks of core stability exercises in female athletes with and without ACL injury. Sport Sciences for Health, pp.1-8.
7. Siedentop, D. and Van der Mars, H., 2022.Introduction to physical education, fitness, and sport. Human kinetics.
8. Mishra, N., Habal, B.G.M., Garcia, P.S. and Garcia, M.B., 2024, June. Harnessing an AI-Driven Analytics Model to Optimize Training and Treatment in Physical Education for Sports Injury Prevention. In Proceedings of the 2024 8th International Conference on Education and Multimedia Technology (pp. 309-315).
9. Pleša, J., Kozinc, Ž. and Šarabon, N., 2022. A brief review of selected biomechanical variables for sport performance monitoring and training optimization.Applied Mechanics,3(1), pp.144-159.
10. Roupa, I., da Silva, M.R., Marques, F., Gonçalves, S.B., Flores, P. and da Silva, M.T., 2022. On the modeling of biomechanical systems for human movement analysis: a narrative review.Archives of Computational Methods in Engineering,29(7), pp.4915-4958.
11. Li, S., Wang, C. and Wang, Y., 2024. Fuzzy evaluation model for physical education teaching methods in colleges and universities using artificial intelligence. Scientific Reports, 14(1), p.4788.
12. Yamasaki, T., 2023. Preventive strategies for cognitive decline and dementia: benefits of aerobic physical activity, especially open-skill exercise. Brain Sciences, 13(3), p.521.
13. Agbaje, A.O., 2023. Associations of accelerometer-based sedentary time, light physical activity and moderate-to-vigorous physical activity with resting cardiac structure and function in adolescents according to sex, fat mass, lean mass, BMI, and hypertensive status. Scandinavian Journal of Medicine & Science in Sports, 33(8), pp.1399-1411.
14. Kaggle. Injury Prediction for Competitive Runners.Available online:https://www.kaggle.com/datasets/shashwatwork/injury-prediction-for-competitive-runners?select=day_approach_maskedID_timeseries.csv. (accessed on 2 June 2024).
15. She, H., 2023. Application of Big Data Analysis in Model Construction to Prevent Athlete Injury in Training. Applied Mathematics and Nonlinear Sciences, 9(1).
16. Zhan, C., 2024. Application of artificial intelligence in the development of personalized sports injury rehabilitation plan. Molecular & Cellular Biomechanics, 21(1), pp.326-326.